Wood Material Science & Engineering
Publication details, including instructions for authors and subscription information:
http://www.tandfonline.com/loi/swoo20

Restoration of exact design for partial compression perpendicular to the grain

T.A.C.M. Van Der Put [a]

[a] Faculty of Civil Engineering and Geosciences, Timber Structures and Wood Technology, Delft University, Delft, The Netherlands

Available online: 30 Apr 2012

To cite this article: T.A.C.M. Van Der Put (2012): Restoration of exact design for partial compression perpendicular to the grain, Wood Material Science & Engineering, DOI:10.1080/17480272.2012.681703

To link to this article: http://dx.doi.org/10.1080/17480272.2012.681703

Wood Material Science and Engineering
2012, 1–12, iFirst article

Taylor & Francis
Taylor & Francis Group

ORIGINAL ARTICLE

Restoration of exact design for partial compression perpendicular to the grain

T.A.C.M. VAN DER PUT

Faculty of Civil Engineering and Geosciences, Timber Structures and Wood Technology, Delft University, Delft, The Netherlands

Abstract
To correct the empirical design rules for locally loaded beams and blocks of Eurocode 5, the theoretical explanation of these rules and of the applied test data is given. It appears that the design rule may be far too conservative, or too unsafe in other cases, and only approximately applies for thin long bearing blocks and not for the short test specimens and support stresses of beams. The theory of the determining influence of load spreading possibility on the strength is verified by all other sufficient extended investigations leading to simple and reliable design rules.

Keywords: *Timber, limit state analysis, failure criterion, compression strength of locally loaded blocks, stress spreading model of the triaxial compression strength based on shear failure of the matrix..*

1. Introduction

As all other Building Regulations, now and in the past, the Dutch Code is based on theory and thus satisfies the by law demanded calculable sufficient reliability. This however changes due to introduction of the newly revised Eurocode 5 rules. Although the theoretical analytical approach of structural analysis is always possible in the form of lower and upper bound limit analysis and is prescribed as basis for design also for the Eurocode, there is a strong tendency to replace theory by arbitrarily extrapolated empirical design equations. Since the extrapolated empirical rule is never identical to the theoretical description, it is always possible and necessary to show, by theory, when an empirical design rule is unacceptably unreliable. This has already started for the new rules of the Eurocode 5 (as reported to the Dutch Eurocode 5 committee). Examples of abandoned theoretical approaches, which were initially accepted by CIB-W18 Eurocode 5 Committee members are for example: van der Put (1990a, 1990b, 1991 and 1993), as will be shown later. In this article, the replacement of theory by unsafe and uneconomical empirical rules will be shown for design of locally loaded beams and blocks to make necessary corrections possible. This was already started by comparison of theoretical with empirical results (within the very limited range of applicability of the empirical rules) by Leijten and Schoenmakers (2007) and Larsen *et al.* (2008). In this article, further the necessary theoretical explanation of the meaning of the applied empirical Eurocode 5 rules is given and the necessary theoretical explanation of the too limited data on which these rules are based.

First in Section 2, the necessary derivation of the empirical Eurocode rule, Equation 1, of Blass and Görlacher (2004) is given, leading to a new explanation of this empirically applied equation; which is based on the derivation of Madsen (see Madsen *et al.* 1982) discussed in Section 2.3. Next, in Section 3, the necessary theoretical analysis of the applied test results is given, followed in Appendix A by a retrieval of the earlier proposed; theory based, Code rules which are in accordance with all known data and are applied since long in many countries.

The empirical Madsen equation is shown in Section 2 to apply only approximately for thin long bearing blocks. This equation, thus, cannot be applied in general as design and Eurocode rule.

Correspondence: T. A.C.M. van der Put, Faculty of Civil Engineering and Geosciences, Timber Structures and Wood Technology, Delft University, TU Delft, P.O. Box 5048, 2600 GA Delft, The Netherlands. Tel: 31 152 851980. E-mail: vanderp@xs4all.nl

(Received 25 January 2011; revised 12 March 2012; accepted 19 March 2012)

ISSN 1748-0272 print/ISSN 1748-0280 online
http://dx.doi.org/10.1080/17480272.2012.681703

Further, it is adapted to the test-results of a too short standard ASTM specimen, given by Case 3 of Figure 1, and to the theoretically nearly as strong variant, Case 2 of Figure 1. This standard test is incorrectly regarded to be representative for all cases in practice, independent of the dimensions of the block and thus independent of the possibilities of stress spreading into the block. This means for example that line 3 in Figure 2, which is comparable with the dimensions of the ASTM test (when performed on an uncut block by a constant loading rate test), replaces all other lines of Figure 2 in the Code. This is of course unacceptable from an economical point of view because of the higher possible strengths of lines 4–7; and is also unacceptably unsafe for the boundary conditions (block dimensions) of the lines below line 3 of Figure 2. In contrast, it is shown by Table II of Section 3.1 that all strengths of all loading lines of Figure 2 follow precisely from plasticity theory discussed in van der Put (2008a). This leads to the necessary application of the given, simple (internationally applied) design rules in Appendix A, covering not only line 3, but all lines 1–7 in Figure 2 precisely and covering all the different lines of the other investigations as shown in van der Put (1991) for the old Eurocode and French rules and for the measurements of Suenson and Graf, given in Kollmann (1984) and Korin (1990). Thus, the apparent contrary and totally different empirical results of all these different investigations are fully explained even by the simple power law representation of the exact theory of e.g. van der Put (2008, 2008a,b) and van der Put and Leijten (2000). This theory is based on the solution of the continuum mechanics boundary value problem of the differential equations of equilibrium, expressed in characteristics, which satisfy the failure criterion. The theory is also shown to be predictive (as a theory should be) and therefore all data of investigations since 1991 and surely also the superfluous future measurements are fully explained. This of course also applies for the Eurocode data of Blass and Görlacher (2004) as shown in paragraph 3.1 for locally loaded blocks and in paragraph 3.2 for locally loaded beams. The reliable and economical design method, based on theory, demanded by European law, thus exists and is given in Appendix A.

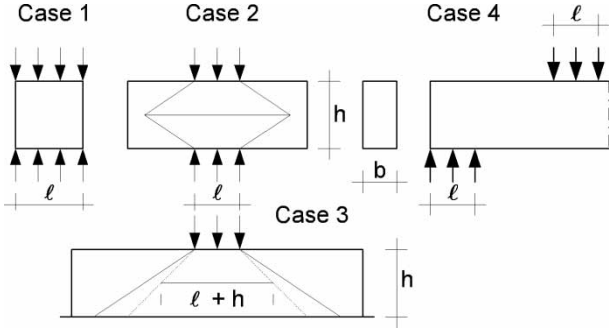

Figure 1. Loading cases perpendicular to the grain of Blass and Görlacher (2004).

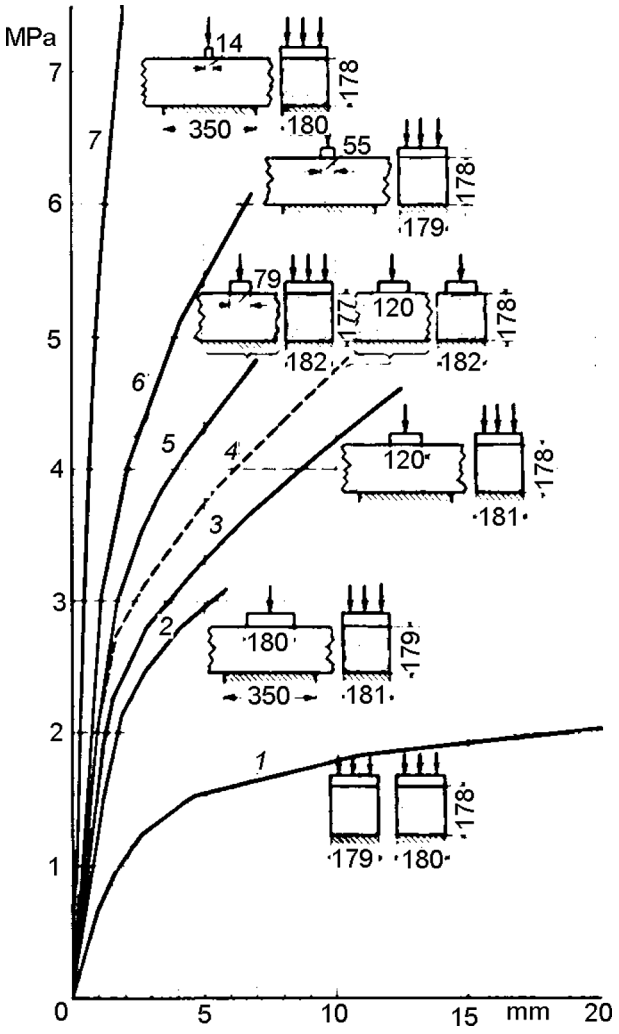

Figure 2. Strength of locally loaded beams of Kollmann (1951, 1984).

2. Derivation of the empirical design equation for locally loaded members

2.1. Derivation of the equation parameters

Generalised empirical rules, which are not explained by theory, are not allowed in design and in regulations because of the unknown applicability and reliability. Therefore, the derivation of the now prescribed empirical design equation first has to be given. Using, in this section, the same notation as Blass and Görlacher (2004), for their design equation based on the equation of Madsen *et al.* (1982),

for locally applied compression perpendicular to the grain, which is:

$$F_{\text{ult}} = A \cdot b \cdot \ell + C \cdot b \tag{1}$$

where A and C are called 'constants' depending on deformation and species, b is the load contact length perpendicular to the grain and ℓ is the contact length parallel to the grain (see Figure 1). Equation 1, based on the theory of elasticity, can be explained as follows:

The deformation Δh of the upper bearing plate with respect to the bottom plate of Case 3 of Figure 1 can, as in practice, approximately be based on the mean stress σ at the mean area $b(\ell + h)$ of all cross sections of the spreading stress, thus:

$$\Delta h = \varepsilon \cdot h = \frac{\sigma \cdot h}{E'} = \frac{F \cdot h}{E' \cdot b \cdot (\ell + h)} \tag{2}$$

Due to confined dilatation, a tri-axial stress state is possible providing a high strength under the loading plate and at flow, this ultimate stress is the highest in the middle under the plate and there is always tri-axial stress spreading into the specimen. The spreading area is such, that the load F divided by the spreading area is equal to the theoretical stress according to theory of elasticity which is the largest in the middle under the plate. This applies at any spreading depth below the plate. The deformation Δh thus follows approximately from the deformation of the spreading pyramid. With the x-axis along the pyramid axis is the area of a cross section at a distance x from the top $c_1x \cdot c_2x = c_1c_2x^2$ and

$$\begin{aligned}\Delta h &= \int_{x1}^{x2} \varepsilon \mathrm{d}x = \int_{x1}^{x2} (P/(EA))\mathrm{d}x = \int_{x1}^{x2} \left(P/(Ec_1c_2x^2)\right)\mathrm{d}x \\ &= (P/Ec_1c_2)(1/x_1 - 1/x_2) \\ &= (P/(Ec_1c_2x_1x_2))(x_2 - x_1) = (P/EA_m)h\end{aligned}$$

because $c_1c_2x_1x_2 = c_1c_2(x_m - \Delta)(x_m + \Delta) = c_1c_2\ (x_m^2 - \Delta^2) \approx c_1c_2x_m^2 = A_m$, the mean area of the spreading frustum. The ultimate value of the mean spreading stress thus gives the start of flow in the middle under the loading plate.

The deformation in the elastic state follows from the plane stress state of Figure 1 by integration of the local strain, assuming a stress spreading of 45°, because then the mean spreading stress is equal to the theoretical maximal reaction stress in the middle under the loading plate as given in Figure 1, Case 3.

Thus, the right deformation according to elasticity theory is,

$$\begin{aligned}\Delta h &= \int \frac{F/E_{90}}{b(l+2h)}\mathrm{d}h = \frac{F}{2bE_{90}} \int \mathrm{d}(\ln(l+2h)) \\ &= \frac{F}{2bE_{90}}(\ln(l+2h) - \ln(l)) = \frac{F}{2bE_{90}} \ln\left(1 + \frac{2h}{l}\right)\end{aligned}$$

According to the elastic–plastic approach of Limit Design this deformation has to be equal to the ultimate value of Equation 2 for an ultimate lower bound solution of the strength. Thus:

$$\begin{aligned}\Delta h &= \frac{F}{2bE_{90}} \ln\left(1 + \frac{2h}{l}\right) \\ &\approx \frac{F}{bE'(l+h)}, \text{ leading to Equation 3 :}\end{aligned}$$

$$E' = \frac{E_{90} \cdot 2h}{(\ell + h) \cdot \ln(2h/\ell + 1)} \approx 0.9 \cdot E_{90} \tag{3}$$

or E' is $(0.83\text{–}0.96) \cdot E_{90}$ for Case 3 when $h/\ell = 0.5 - 2$. For loading Case 2: $E' = E'' = 0.96 \cdot E_{90}$ or $(0.91\text{–}0.99) \cdot E_{90}$ when $h/\ell = 0.5 - 2$. Of course, the precise value of E' instead of $0.9 \cdot E_{90}$ can be used in Equation 3 for a special h/ℓ value.

Equation 2 can be written for Case 3:

$$\begin{aligned}F &= \frac{\Delta h}{h} \cdot E' \cdot b \cdot (\ell + h) = \frac{\Delta h \cdot E' \cdot b \cdot \ell}{h} + \Delta h \cdot E' \cdot b \\ &= A \cdot b \cdot \ell + C \cdot b\end{aligned} \tag{4}$$

Herewith the meaning of A and C in Equation 1 are derived:

$$\begin{aligned}A &= \Delta h \cdot E'/h = \varepsilon \cdot E' \text{ and } C = \Delta h E' \\ &= \varepsilon \cdot E' \cdot h \text{ and } C/A = h\end{aligned}$$

Substitution into Equation 1 gives:

$$F_{\text{ult}} = A \cdot b \cdot \ell + C \cdot b = \varepsilon_u E' b(\ell + h) = Ab(\ell + h). \tag{5}$$

The strength, thus, is based on a measured ultimate strain ε_u under the load. This has to be explained further and follows from the exact solution of Section 2.2.

According to Eurocode 5 Equation 1 is:

$$\begin{aligned}F_{\text{ult}} &= A \cdot b \cdot \ell + C \cdot b = Ab(\ell + C/A) \\ &= Ab(\ell + 0.3).\end{aligned} \tag{6}$$

Thus, against the data of Figure 2, the strength of 30 mm high blocks is regarded to always apply for all dimensions and spreading possibilities. The real ultimate load depending on the spreading possibility follows from the theory given in complete form in van der Put (2008a), which is applied in Sections 2.2 and 3.

2.2. Theoretical explanation of the Madsen equation

The strength according to the empirical Madsen equation should be explainable by the exact theory of limit analysis. According to van der Put (1991, 2008a), the real theoretical ultimate stress $F_{ult}/b\ell$, as follows from the equilibrium method of plasticity, can be given as:

$$\sigma_{\text{ult}} = F/b\ell = 1.1 \cdot f_{c,90}\sqrt{A_s/A_0}, \tag{7}$$

where $f_{c,90}$ is the compression strength perpendicular to grain given by Figure 4 and $A_0 = b\ell$ is the area of the contact surface of the upper loading in Figure 1, Case 3, and A_s the area of the spread stresses with a slope of 1 to 1 when initial flow, the start of plastic strain of the Codes, is chosen as the ultimate state. Thus $A_s = b(\ell + 2h)$ for Case 3, and from Equation 7 follows:

$$\begin{aligned} F_{\text{ult}} &= \sigma_{\text{ult}} A_0 = 1.1 \cdot f_{c,90} \cdot A_0 \sqrt{A_s/A_0} \\ &= 1.1 \cdot f_{c,90} \cdot \sqrt{A_s \cdot A_0}. \end{aligned} \tag{8}$$

As applied previously for the derivation of Equation 2, the Madsen equation for the middle plane A_m is:

$$\begin{aligned} \sigma_m A_m &= 1.1 \cdot f_{c,90} \cdot \sqrt{A_s \cdot A_0} \\ &= 1.1 \cdot f_{c,90} \cdot \sqrt{(A_m + \Delta) \cdot (A_m - \Delta)} \\ &= 1.1 \cdot f_{c,90} \cdot \sqrt{A_m^2 - \Delta^2} \approx \\ &\approx 1.1 \cdot f_{c,90} \cdot A_m (1 - \Delta^2/2A_m^2) \\ &\approx f_{c,90} \cdot A_m, \text{ or : } \sigma_m \approx f_{c,90} \end{aligned} \tag{9}$$

In these equations $A_m = b(h + \ell)$ and $\Delta = bh$, the difference between the maximal and minimal spreading area. Equation 9 applies when $\Delta^2/2A_m^2 \ll 1$, thus for $\ell \gg h$. Then, for $\ell = (1-2) \cdot h$ follows: $1.1\left(1 - \Delta^2/2A_m^2\right) = 1.1 - 1.1(bh)^2/(2b^2(h+l)^2)$ $= 1.1 - 1.1/(2(1 + l/h)^2) = (1.1 - 1.1/8)$ to or : $= 0.96 - 1.04$. Thus $\sigma_m \approx (0.96\text{–}1.04) \cdot f_{c,90}$.

Thus, the Madsen equation can be interpreted as the requirement that the mean stress σ_m at the mean elastic spreading area A_m, at the middle of the depth, should be lower than $f_{c,90}$. This explains the derivation and design method of Section 2.1 and determines ε_u of Equation 5.

It is now shown that the Madsen equation (with $C/A = h$) only applies approximately for small spreading possibilities when the load contact length ℓ is higher than the bearing block depth h. This result shows that there is no possibility to generalise empirical rules outside the dimensions and conditions of testing without a theoretical analysis.

2.3. Derivation by Madsen et al.

Because the background of the prescribed design equation, the Eurocode 5 rule Equation 1 is not sufficiently reported, it is discussed here. Equation 1 is derived for example in Madsen *et al.* (1982), adapted to tests results on standard blocks as given in Figure 3. From elastic finite element analysis follows that for sufficient long blocks, the deformation and thus the stress is zero at a distance $L_D \approx 1.5 \cdot H$.

The spreading action of the upper layers of the beam of that length was modelled as a fractional beam on elastic foundation with depth d, and foundation modulus $k = E_{90}b/H$, based on the compressibility and thus on the compression modulus perpendicular to the grain of the block. The bending stiffness of the fractional beam is $EI = E_0 bd^3/12$ where E_0 is the modulus of elasticity in the longitudinal direction of the block. The depth $d = 0.17H$ was found to duplicate the finite element results of the deformation of the upper surface, because this would be the deformation of the loaded separate fractional beam of depth d at this elastic foundation The characteristic length is: $\lambda = \sqrt[4]{4EI/k} = 0.2H(E_0/E_{90})^{0.25}$ and the location of zero reaction on the fractional beam thus is: $L_D = 3\lambda = 1.6H$, slightly higher than the theoretical $1.5H$. Because the displacement of the upper layer $\delta L_D/3$, given by the dashed, area in Figure 3, determines the embedment reaction on the fractional beam, the end shear of the beam will be: $k\delta L_D/3 = 0.53\sigma_{90}bH$ and from vertical equilibrium of the beam follows:

$$F_u = \sigma_{90,u} b(l + 1.06H) \tag{10}$$

confirming the elastic-full plastic solution $F_u = \sigma_{90,u} b(l+H)$ derived in Section 2.1.

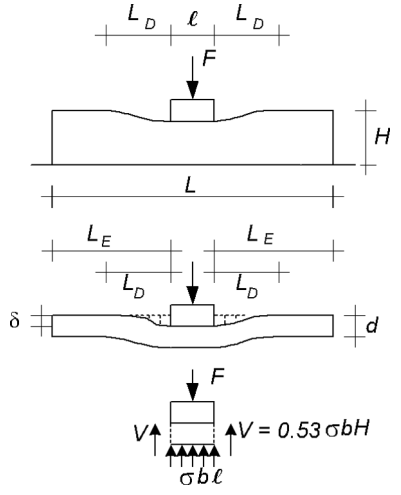

Figure 3. Basic central compression test of Madsen *et al.* (1982).

For the solution for short, high, blocks a limited depth H' applies for $L_D/15$ instead of the empirically adapted value of Madsen, giving a too low strength. Thus, when regarded as a Limit Design solution, Madsen's adaptation gives a too low lower bound solution of the strength.

For inelastic analysis, elastic full-plastic finite element analysis was applied, leading to an elastic foundation model with hinges at the loading plate, (according to the kinked deformation of the upper surface of the block adjacent to the bearing plate). This leads to half the value of the dashed area of Figure 3, and thus to an end shear of $0.265\sigma_{90}bH$ or:

$$F_u = \sigma_{90,u} b(l + 0.53H). \tag{11}$$

This solution thus also gives a too low lower bound of the strength. Madsen replaced $0.53D$ by 30 mm, indicating the depth H of his standard test blocks to be: $H = 30/0.53 = 57$ mm. Because the highest found lower bound solution is the closest to/or equal to the real solution, the higher and thus more probable lower bound follows from the solution of Section 2.1: $F_u = \sigma_{90,u} b(1+H)$.

This determining solution thus implicitly is applied as: $F_u = \sigma_{90,u} b(1+30)$ as Eurocode rule, and thus is it assumed that all structures and bearing blocks have a depth of 30 mm and the lengths L of the bearing blocks (or distance between applied loads) is higher than $L \geq l+3H = l+90$ mm mm (as necessary for confirmation of the spreading according to the theory of Section 3.1 and according to the beam on elastic foundation model). However, much shorter blocks, that do not apply to Equation 1, were tested for Eurocode 5 data. These short blocks thus mutually show the same spreading length for all test specimens and thus the influence of spreading according to the beam on elastic foundation theory is not tested. Table I shows that only one spreading case (because of the same dimension ratios) is tested. The Eurocode rule thus cannot apply generally for all possible dimensions as given in Figure 2 but may possibly apply, when properly adapted, to one case of Figure 2, (roughly line 3 of Figure 2).

Table I. Strength reduction factors with respect to full spreading of Figure 1 data.

Case	Depth h (mm)	Spreading R	Friction S	Strength $R \times S$	Data $R \times S$
2	200	1.0	1.0	1.0	1.0
3	200	1.0	1.0	1.0	1.0
2	100	0.9	1.1	1.0	1.0
3	100	1.0	1.1	1.1	1.1
2	50	(0.76)	1.2	0.9/10	1.0
3	50	(0.9)	1.2	(1.1)/ > 1.0	1.0

Notes: $R = 1$ means spreading over the full length of the specimen. Brackets on the frictionless values according to Figure 5, means higher strength according to Figure 6 by friction along the loading plates.
Case 2, Equation 15 and Case 3, Equation 16.

3. Explanation of the Eurocode 5 strength test data for locally compression perpendicular to the grain

3.1. Strength analysis of bearing blocks data

The expected strength values of the pure compression tests according to Case 1 of Blass and Görlacher (2004), given in Figure 4, with loading area $b \cdot \ell = 120 \cdot 100\,\text{mm}^2$ and $h = 50$, 100 and 200 mm are the same, because the critical slip line will have an angle of about 45°, showing the same dissipation for all three depths at movement along these slip-lines. However, when the friction along the loading plates is determining, a fainter slope (dashed line in Figure 4) is enforced, causing a higher strength of the specimen with $h = 50$ mm. The fact that Cases 2 and 3, of Figure 1, show a minor influence of the depth, is due to the chosen small axial length and thus the small spreading length of the test specimens. For these cases, the beam length is 300 mm and the loading area is also $120 \cdot 100$ mm^2 with $h = 50$, 100 and 200 mm. As in the tests of Korin (1990), the specimen length (of 300 mm) limits the spreading length and because of the same full spreading lengths, there is no difference in strength for Case 3, of Figure 1, between specimens with $h = 100$ and $h = 200$ mm. Korin's results were discussed in van der Put (1991) and if the there given old exact Eurocode Design rules had been followed, the unnecessary test series could have been avoided.

As mentioned in Section 2.2, Equation 7, the real theoretical ultimate stress, is: $\sigma_{\text{ult}} = F/b\ell = 1.1 \cdot f_{c,90}\sqrt{A_s/A_0}$, where $A_0 = b\ell$ is the contact area of the upper loading in Figure 1, Case 3, and A_s, the area of the spread stresses at the bottom, is found by a spreading slope of 1.5–1 as applies for

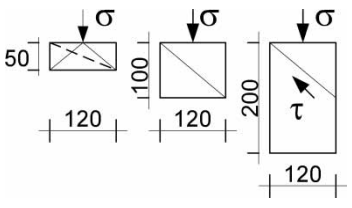

Figure 4. Compression tests of Blass and Görlacher (2004).

the ultimate state after sufficient plastic flow. Thus for Case 3:

$$A_s = b(\ell + 3h) \tag{12}$$

and $A_s = b(\ell + 3h/2)$ for Case 2. The spreading length is limited by full spreading, thus is at the maximum equal to the specimen length of 300 mm, $\ell + 3h \leq 300$ and $\ell + 3h/2 \leq 300$, where h ($=h'$ in Figure 1) now is the spreading depth, giving:

$$\begin{aligned}\text{Case 3}: \sigma_{\text{ult}} &= \frac{F_{\text{ult}}}{b\ell} \\ &= 1.1 \cdot f_{c,90}\sqrt{\frac{\ell + 3h}{\ell}} \leq 1.1 \cdot f_{c,90}\sqrt{\frac{300}{100}} \\ &= 1.1 \cdot f_{c,90} \cdot 1.73 \\ &= 1.9 \cdot f_{c,90}\end{aligned} \tag{13}$$

$$\text{Case 2}: \sigma_{\text{ult}} = \frac{F_{\text{ult}}}{b\ell} = 1.1 \cdot f_{c,90}\sqrt{\frac{\ell + 3h/2}{\ell}} \leq 1.9 \cdot f_{c,90} \approx 1.9 \cdot 4 = 7.6 \text{ MPa} \tag{14}$$

Due to the maximal spreading length of 300 mm, the ultimate strength is: 7.6 MPa. The best estimate of the compression strength is: $f_{c,90} = 4$ MPa. This has to be measured in this case on the same specimen dimensions as Case 3, with a rigid bearing plate over the full length of the specimen. The best alternative form in this case is given by the cube test of Blass and Görlacher (2004) with $h = 50$ mm, giving a strength of about 4 MPa. In Table I, the strength is given by a reduction factor R with respect to the maximal value of 7.6 MPa (of the specimens with full spreading over 300 mm) according to Equations 14 and 13:

$$\text{Case 2}: \text{Spreading factor}: R = \sqrt{(2\ell + 3h)/600} = \sqrt{(200 + 3h)/600} \leq 1 \tag{15}$$

$$\text{Case 3}: \text{Spreading factor}: R = \sqrt{(\ell + 3h)/300} = \sqrt{(100 + 3h)/300} \leq 1 \tag{16}$$

Full spreading is reached for $h > 133$ for Case 2, and $h > 67$ for Case 3. Therefore, the first two rows of Table I only show the value 1.0. The influence of higher strengths of the lower specimens due to friction along the bearing plates follows from the ratio of strengths of the Case 1 compression strength tests with respect to the $h = 200$ mm data, being: $S = 4.1/3.4 = 1.2$ for $h = 50$ mm; $S = 3.7/3.4 = 1.1$ for $h = 100$ mm in Table I.

The values of R of Table I are based on the maximum shear lines of Figure 5 of no friction at the bearing plates. For specimens of 50 mm depths, these reduction factors are placed between brackets, because also the shear lines according to Figure 6 are possible by friction, because the loading plate length of ℓ=100 mm is higher than the depth $h = 50$ mm. The shear (or slip-) line field of Figure 6 is identical to the slip line field of Case 2 of Figure 1 for $h = 100$ mm, giving the same dissipation for movements along slip lines and thus the same strength. Further, for relative long plates, this slip line field may occur as well in Cases 2 and 3, giving mutual the same theoretical strengths of 50 mm specimens, leading to the reduction factor $(R \times S) = 1$ for $h = 50$ mm in Table I. The brackets in Table I, thus, mean that the strength according to Figure 6 and not according to Figure 5 is determining.

It is now shown that the chosen special dimensions in Blass and Görlacher (2004), with minor stress spreading possibilities of the test specimens, are causing the minor difference between Cases 2 and 3 and the minor influence of the member depth on the strength as given in Table I. This is totally different from the results of Figure 2, where the total range of stress spreading possibilities is measured and the strength may be six times higher with respect to the Case 1 compression strength (when local failure is determining). It is shown in van der Put

Table II. Stress spreading factor: $k_{c,90} = \sigma_{c,90,u}/f_{c,90} = 1.1 \cdot \sqrt{0.5 + 442/s}$ of Figure 2 data.

	1	2	3	4	5	6
Curve of Figure 2	S (cm)	$f_{c,90}$ (MPa)	$k_{c,90}$ Equation 18	Theory $\sigma_{c,90,u}$ (MPa)	Measurements $\sigma_{c,90,u}$ (MPa)	Ultimate strain 6/178 (%)
1	18	1.6		1.6	1.6	3.4
2	18		1.89	3.0	3.0	3.4
3	12		2.25	3.6	3.3	3.4
5	7.9		2.72	4.3	4.3	3.4
6	5.5		3.21	5.2	5.4	3.4
7	1.4		6.23	10 < 9.6	> 7.5	> 1

Notes: Columns 4 and 5 show a precise fit of data to the spreading theory.
Curve 7 is cut off at 7.5 MPa in Figure 2. The theoretical value of 10 MPa is not met by the local failure mechanism: $\sigma_{c,90,u} \leq 6$.
$f_{c,90} = 6.1.6 = 9.6$ MPa.

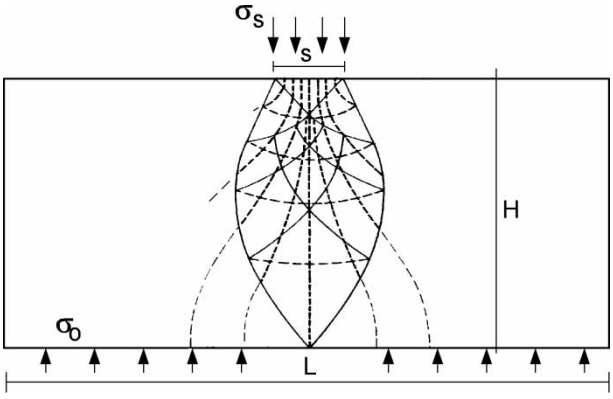

Figure 5. Ultimate shear line construction.

(1991, 2008a) and by Table II, that the strengths of all loading lines of Figure 2 follow precisely from theory giving:

$$k_{c,90} = \frac{\sigma_{c,90,u}}{f_{c,90}} = 1.1 \cdot \sqrt{\frac{L'}{s}} = 1.1 \cdot \sqrt{0.5 + \frac{3H + L}{2s}} \leq 6 \tag{17}$$

where the notations are given in Figure 7. With $H = 179$; $L = 350$ and $b = 181$ mm:

$$k_{c,90} = 1.1 \cdot \sqrt{0.5 + (3 \cdot 178 + 350)/2s} = 1.1 \cdot \sqrt{0.5 + 442/s} \tag{18}$$

These compression strength values σ_{c90u} according to the theory are given in Table II column 4, together with the measurements in column 5, showing a nearly perfect match. Due to possible splitting of the test-specimen, the end-point of line 2, 5 and 6 in Figure 2 are chosen at about 6 mm. This always possible value of 6 mm, thus, is also taken as ultimate value for the other cases of Figure 2. The theory leads to real reliable very simple Eurocode rules as given in Appendix A. Because these rules or the consequential high strength already has been applied since decades, it is a serious obstruction for building possibilities to lower this value strongly as is done in the new proposal for the Eurocode.

3.2. Strength analysis of locally loaded beams data

Only for loads directly adjacent to the support, the failure mechanisms of locally loaded blocks and

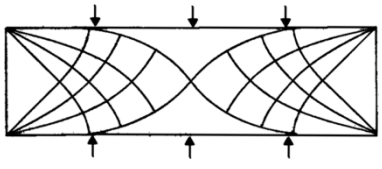

Figure 6. Compression test.

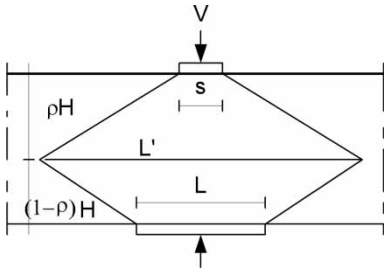

Figure 7. Partial loaded and supported block.

locally loaded beams are comparable (van der Put 1991), making it possible to use the same design rules (as then proposed in 1991 for the Eurocode). This applies when the bottom plate at the support and upper loading plate overlap. (see 9 and 10 of van der Put and van de Kuilen (2009)). At larger distances of the load to the support, spreading to the opposite free surface is possible when a tensile stress field is superposed. This tensile field is normally not determining for failure except for middle supports of continuous beams due to the interaction with shear and bending stresses at failure. This is derived in van der Put and van de Kuilen (2009) leading to a design method, including continuous beams, which, besides moment redistribution by plastic flow in bending, may show a plastic shear flow mechanism also causing a full moment redistribution. The derivations show how the shear stress may reduce the ultimate bending capacity. Because failure at the middle support should be by bending and shear and should not occur earlier by compression perpendicular to the grain, the simple Code requirement is possible, that the load-bearing plate length $\ell \geq 0.64h$ for not overlapping bearing plates. For the middle support reaction of the continuous beam, twice this value applies. This requirement follows for loads close to the support from the determining case of loading directly adjacent to the support to prevent shear failure of the beam at the ultimate compression stress due to spreading of about 2 $f_{c,90}$ on the loading plate (see van der Put and van de Kuilen 2009).

The failure analysis of Case 4 of Figure 1, of the data of Blass and Görlacher (2004) for locally loaded beams, probably on two supports, is difficult here because no information is given on the true loading curves and on the distance between the applied load and supports or other boundary conditions at the loading end, etc. It is further not defined what the 'projecting member end', the 'measuring length' etc. is. Stated is also that $\xi = 1$, meaning ℓ to be infinite, despite the finite lengths of the bearing plates. However, Table III of Blass and Görlacher (2004), here also included as Table III, extended with the

Table III. Failure mode of Figure 1, case 4 tests on beam ends.

Case 4 Figure 1	1 number	$2h$	$3b$	4ℓ	5 shear h/ℓ	6 compression $\sim F/F_{u,4}$	7 + spreading $\sim F_{u,s}/F_{u,4}$
Series 1	6	320	120	120	2.67	(1.8)	$(1.8 \times 2.23 = 4.0)$
Series 2	4	630	120	240	2.63	(3.6)	
Series 3	4	700	220	280	2.5	(7.7)	
Series 4	5	1000	100	80	(12.5)	1	$1.0 \times 4.4 = 4.4$
Series 5	10	540	120	90	(6.0)	1.35	$1.35 \times 3.16 = 4.3$

Notes: A value ~ 2.6 in column 5 means shear failure.
A value ~ 1 in column 6 means compression perpendicular failure.
Column 7 gives column 6 times the spreading factor $\sqrt{1 + 1.5h/\ell}$ showing series 4 and 5 to be equally strong.

determining factors, gives sufficient indication on the type of failure.

Since the by Blass and Görlacher (2004) measured ultimate loads are about of the same order, it is certainly impossible that, the compression strength perpendicular to the grain is always the cause of failure, as supposed by Blass and Görlacher (2004), because the ultimate compression stress (at flow) on the bearing plate of 220×280 (series 3) is a factor 7.7 lower than for the plate of 80×100 (series 4), showing thus no failure by compression and therefore the strength factor 7.7 in Table III, column 6 is placed between brackets. The stress is a factor $1/(7.7) = 0.13$ too low for compression failure. Similarly, the by a factor 1.8 and 3.6 measured lower compression stresses of series 1 and 2 are placed between brackets. Compression failure has to be excluded for these cases. Bending failure also has to be excluded. Even series 1 of Table III was strong enough to fail by shear, thus for e.g. series 5 the bending stress is at least a factor $(120/100)/(320/1000)^2 = 0.12$ too low for bending failure. Further, if in a three-point bending test, the distance between the midpoint loading F and reaction R is a, then the moment is: $R \cdot a = F \cdot a/2 = f_m bh^2/6$, giving:

$$\frac{F}{b\ell} = \frac{h}{\ell} \cdot \frac{f_m}{3a/h} \tag{19}$$

If the ultimate bearing stress $F/b\ell$ is of the same order (as measured) for the series, then $h^2/a\ell$ must be constant for bending failure, which is not the case because only h is varied in the tests series. Thus, shear failure remains as possible cause of failure for the beams with large bearing plates (series 1–3 in Table III). This is the common failure type for loading near the support. For shear failure due to the reaction force R:

$$\frac{R}{2bh/3} = f_v = \text{const. or } \frac{F}{bh} = \text{const. thus : } \frac{F}{b\ell} = \frac{h}{\ell} \cdot \text{const.} \tag{20}$$

Thus, when the compression stress on the bearing plate F/bl is about the same for all series, then also h/l has to be the same when shear failure is the cause of failure. This applies for series 1–3, as can be seen in column 5 of Table III showing the same $h/\ell \approx 2.6$. Clearly, shear failure does not apply for series 5 and 4 showing too high factors of 12.5 and 6.0 which would show a higher strength by a factor $6/2.6 = 2.3$ and $12.5/2.6 = 4.8$. Thus, only these series 4 and 5 with small loading plates show early failure by compression alone. For series 4 is as a first estimate:

$$F_{u,4} = \rho f_{c,90} b\ell = \rho f_{c,90} \cdot 100 \cdot 80 \tag{21}$$

and for the same order of the ultimate load F_u and the same spreading factor ρ $F/F_{u,4} \approx b \cdot \ell/100 \cdot 80$. This strength factor, relative to the strength of series 4, depending on the dimension of the loading plate is given in column 6, showing that only series 4 and 5 show the high compression failure stress and not for example series 3, which then shows a factor $1/7.7 = 0.13$ too low stress for compression failure. At sufficient distance between the loads, the spreading factor on the compression strength ρ is for spreading in one direction similar to Equation 13: $\sqrt{((\ell + 1.5h)/\ell)}$, for high beams and the by this factor multiplied relative strengths of column 6, are given in column 7. This means that series 4 and 5 are about equally strong. This is confirmed by the stress–strain diagrams of Blass and Göerlacher (2004) at an ultimate strain of 0.04. These curves also show that the shear strengths of series 1–3 are according to the given factors in column 5. Thus, the strength of series 1 is a factor $2.67/2.5 = 1.07$ higher with respect ot series 3. Because some specimens of series 1 show early flow in compression (thus at a stress of $1/1.8 = 0.55$ times the ultimate stress) and because of the measured long hardening range, it is possible that series 1 also failed by compression perpendicular to grain. In that case, the ultimate strength of series 1 is a factor $4.0/4.4 = 0.9$ lower with respect to series 4 and 5 at the ultimate strain of

0.04. This analytical factor of about 0.9 between the strengths of series 1 with respect to series 4 and 5 is confirmed by the data in Figure 4 of Blass and Görlacher (2004). However, series 1 fails primary in shear because the high compression stress at failure does not influence the shear strength which is even a bit higher than those of series 2 and 3.

It could have been predicted by design that series 1–3 are about equally strong and could not fail by compression perpendicular to the grain and by the stress spreading formula that series 4 and 5 are equally strong. Thus, for example, series 4 remains as only information on compression perpendicular failure of beams. However, at failure the bending stress was at least a factor 0.12 too low for bending failure and at least a factor $1/4.8 = 0.21$ too low for shear failure. This information thus is not useful because compression perpendicular should not reduce the bending and shear strength of a beam. Thus, a combined loading mechanism should have been designed and investigated accordingly. Therefore, combined compression – shear strength mechanisms of locally loaded beams and of continuous beams, depending on the dimensions and volume effect, should be analysed by the theory of van der Put and van de Kuilen (2009).

3.3. Serviceability requirement of locally loaded beams and blocks

A demand for design is to guarantee sufficient reliability. This of course also applies for compression strength perpendicular to the grain. This cannot be replaced by a serviceability requirement. Such a requirement is subjective and depends on the type of structure and on the user, and is in the Codes as possible application. Of course, this cannot replace a statutory strength criterion with a guarantied level of safety. Prescribing the application of a serviceability condition, thus, means; prescribing a second always determining non-sense strength criterion which, in this case, prevents building possibility and new future developments. Also, for instance, bracing and prop-up at yacht building etc. is no longer possible. According to this serviceability requirement, all important Dutch cities could not have been build and should now be demolished, although the loading is below the long-duration strength, despite huge deformation of the head-beam over the pile heads of the pile foundation, which is fully pressed together at the pile head during the ages, showing no empty spaces in wood any more.

The consequences of the serviceability limit of the Eurocode (which is independent of specimen dimensions) can be seen by drawing a vertical line in Figure 2 at the proposed 3 mm deformation restriction. This is uneconomical for line 6 and at the same time unacceptably unsafe for line 7 because the allowed serviceability strain is above its ultimate failure strain. If this serviceability 3 mm deformation serves as ultimate strength condition, it should be compared with the lower percentile of ultimate deformation, and then it is unsafe for most of the curves in Figure 2. It is further forbidden to apply this requirement because there is an European agreement (pact) of not excluding reliable European products on national markets by additional serviceability requirement. There, in fact, only a Code strength requirement exists.

4. Conclusions

An explanation and a new meaning is given to the empirical Madsen equation for the partial compression strength perpendicular to the grain, applied by Blass and Görlacher (2004) as Eurocode 5 rule. This equation appears to be a stress–strain relation expressed in the real elastic stress (determining the mean spreading area) in the middle of the bearing block, limiting this stress to the compression strength $f_{c,90}$.

The factor 0.3 of the Madsen/Eurocode equation: $F_{\text{ult}} = Ab(\ell + 0.3)$ has to be replaced by the depth h according to the theoretical meaning of this equation as limitation of the mean elastic stress in the middle of the bearing block in the ultimate state.

The derivation shows that the Madsen equation, when generalised according to rigorous limit theory, applies for limited stress spreading, when the depth of the bearing block h or H is smaller than the length ℓ of the load contact plate and according to Madsen's derivation the length L of the block is higher than $\ell + 2L_D = \ell + 3H$ thus: $L > \ell + 3H > 4H$ and the rule thus is not generally applicable. These requirements for application are not fulfilled by the chosen far too short and thick ASTM-specimens and the Eurocode test data of Blass *et al.* (2004) thus do not apply to the Madsen equation and thus do not verify this Code rule.

Table I shows that, according to theory, no real differences in strengths between Cases 2 and 3 could be expected for the Blass and Görlacher (2004) chosen depths between 50 and 200. The chosen short standard ASTM dimensions of the Eurocode test specimens, with limited stress spreading possibility, causes negligible influence of the depth of the tests.

The determining influence of the stress spreading possibility on the strength is known since long and discussed on several occasion at CIB-W18 meetings (see e.g. van der Put (1991)) and follows e.g. from Figure 2, where the total range of spreading

possibilities is involved. Thus, the general conclusion of Blass and Görlacher (2004) based on the tests of Table I, of no influence of the depth of the specimen on the strength does not hold. Also, the conclusion that this lack of influence means that the serviceability state is measured is not right because their bend down load – displacement curves show that the ultimate state is reached with a high amount of plastic strain, of higher order than the real elastic strain.

Figure 2 (whereof the ultimate values of all lines are explained by theory by one and the same equation with the same compression cube-strength) shows, that the in Blass and Görlacher (2004) proposed limit of absolute deformation at the contact surface to be not more than a few millimetres does not limit the stress to one value independent of dimensions and gives no information about safety and the loading state, which may be the ultimate state or may be far below this ultimate state for other boundary conditions. The design and the Code requirements remain to provide a criterion of sufficient safety against failure. An extrapolated, subjective, serviceability state is thus shown here to give no information on the violation of this reliability.

The local compression strength perpendicular to the grain contains a spreading factor as given in Equations 13 and 14. It has to be accepted for complicated boundary value problems, that the strength contains a geometric factor as applies for example in Fracture Mechanics and by volume effects of shear- tensile- and embedding strengths. The spreading factor accounts for a sufficient high triaxial compression strength by confined dilatation and for a sufficient low ultimate shear stress in the wood matrix.

The spreading theory applies generally, also for for example concrete and for the embedding strength of particle board wherefore an extended verification is given by van der Put (2008b).

It is shown that the lack of knowledge of the spreading effect in Eurocode 5 can be highly unsafe. This already occurred for example by measuring high embedding strengths on specimens with large nail distances and applying this to the low strength structure by small nail distances.

Although the given design rules apply for the whole a Europe, no information is given on the thereupon-based tests on beam ends. Whether it was a three-point or four-point bending test and how it was managed to make the free support determining for failure by shear and not the loading point in combination with bending. This information is needed for theory confirmation.

The design rules for bearing blocks do not apply unconditionally for support stresses in beams. Only for loads directly adjacent to the support, the failure mechanisms of locally loaded blocks and locally loaded beams are comparable. At larger load distances, the area of the bearing plate should be so high that ultimate load according to the spreading mechanism is lower than the adjacent ultimate shear force. Under-dimensioned bearing plates for loads near a middle support of continuous beams also can be prevented by the simple Code requirement of a bearing plate length $\ell \geq 0.64h$ for not overlapping bearing plates (of load and reaction).

Table III (and the data) shows series 4 and 5 with the smallest bearing plates to be the strongest, due to high shear strength. The other beams series 1–3 fail in shear and thus should not have been accounted as compression failure data (giving the wrong design equation for support stresses in the Eurocode).

It could have been predicted by spreading theory that series 4 and 5 of Table III would be equally strong and provide no additional information on the occurred local compression failure, which could have been obtained by testing blocks. Because for example in series 4, the bending and shear stress were respectively 0.12 and 0.21 times the ultimate value, the wanted design value is not measured for combined failure by compression, bending and shear.

Right and reliable design rules, based on theory, covering data of all published investigations, exist and are given in van der Put (1991) and its Appendix B for locally loaded bearing blocks. For locally loaded beams, design should be based on plasticity theory with the failure criterion for combined stresses, given in van der Put and van de Kuilen (2009). Design rules also exist in technical reports of the Stevin laboratory for pin-dowel joints, and in particle board, accounting for the possible very high embedding strength. This is common knowledge already applied for over 30 years.

References

Basta, C. T. (2005) Characterizing perpendicular-to-grain compression in wood construction applications. Master of Science thesis, Oregon State University.

Blass, H. J. and Görlacher, R. (2004) Compression perpendicular to the grain. Available at: http://www.rz.uni-karlsruhe.de/~gc20/IHB/PUBLIC/35.pdf

Bogensberger, T., Augustin, M. and Schickofer, G. (2011) Properties of CLT-panels exposed to compression perpendicular to their plane. CIB-W18/44-12-1. Alghero, Italy.

Kollmann, F. (1984) *Principles of Wood Science and Technology, Vol. 1* (Berlin: Springer Verlag). (1951, pp. 721–736).

Korin, U. (1990) Timber in compression perpendicular to grain. CIB-W18/23-6-1. Lisbon, Portugal.

Larsen, H. J., van der Put, T. A. C. M. and Leijten, A. J. M. (2008) The design rules in Eurocode 5 for compression perpendicular to the grain–continuous supported beams. CIB-W18/41-6-3. St. Andrews, Canada.

Leijten, A. J. M. and Schoenmakers, J. C. M. (2007) Bearing strength perpendicular to the grain of locally loaded timber blocks. CIB W18/40-6-1. Bled, Slovenia.

Madsen, B., Hooley, R. F. and Hall, C. P. (1982) A design method for bearing stresses in wood. *Canadian Journal of Civil Engineering*, 9, 338–349.

van der Put, T. A. C. M. (1990a) Stability design and code rules for straight timber beams. CIB-W18/23-15-2. Lisbon, Portugal.

van der Put, T. A. C. M. (1990b) Tension perpendicular to the grain at notches and joints. CIB-W18/23-10-1. Lisbon, Portugal.

van der Put, T. A. C. M. (1991) Discussion of the failure criterion for combined bending and compression, Appendix a: bearing strength perpendicular to the grain of locally loaded blocks. CIB-W18/24-6-1. Oxford, United Kingdom.

van der Put, T. A. C. M. (1993) Discussion and proposal of a general failure criterion for wood. CIB-W18/26-6-1. Athens, USA.

van der Put, T. A. C. M. (2008a) Derivation of the bearing strength perpendicular to the grain of locally loaded timber blocks. *European Journal of Wood Wood Production*, doi:10.1007/s00107-008-0258-0.

van der Put, T. A. C. M. (2008b) Explanation of the embedding strength of particle board. *European Journal of Wood Wood Production*, doi:10.1007/s00107-008-0234-8. See also: Stevin Report TU-Delft 25-88-63/09-HSC-6 or: EC-project MA1B-0058-NL, 1988, and the theoretical explanation of the strength of nailed particle board to wood connections in: Stevin Reports 4-79-6/HSC-3; 4-80-3/HSC-4; and 4-81-7/HSC-5.

van der Put, T. A. C. M. and Leijten, A. J. M. (2000) Evaluation of perpendicular to grain failure of beams caused by concentrated loads of joints. CIB-W18/33-7-7. Delft, The Netherlands.

van der Put, T. A. C. M. and van de Kuilen, J. W. G. (2009) Derivation of the shear strength of continuous beams. *European Journal of Wood Wood Production*. doi:10.1007/s00107-010-0473-3. Published on line 25 August 2010.

Appendix A: Proposal for design rules for partial compression perpendicular to the grain

The design rules for partial compression perpendicular to the grain, proposed at CIB-W18 of 1990, 1991 and 2000, are based on the theory, published in complete form in van der Put (2008a), providing an excellent explanation and precise fit of all the apparent contradictory test results of Suenson, the old Eurocode, the French rules, Graf, Korin and Augustin *et al.* in all circumstances and loading cases. The CIB-W18 Eurocode proposal for bearing blocks was based, as should be, on the measured ultimate strength according to a spreading slope of 1.5–1. The proposal here is based on the definition of the Regulations of the strength being the stress at the start of initial flow, showing the near elastic spreading slope of 1–1. Then:

$\sigma_{c,90,d} \leq k_{c,90} \cdot f_{c,90,d}$, where:

$$k_{c,90} = \sqrt{L/s} \leq 5 \text{ with : } L \leq a + s + l_1/2; L \leq 2H + s$$

The notations are given in Figure A.1.

For the bearing strength of a middle section of a beam between two plates of lengths L and s:

$k_{c,90} = \sqrt{L'/s} \leq 5$ with: $L' \leq H + L + s/2$; and: ($L' \leq a + s + l_1/2$, the length of the specimen). See Figure 7 (and Figure A1) for the meaning of the notations.

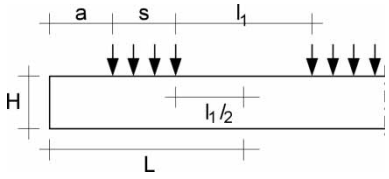

Figure A.1. Continuous supported block with partial loading perpendicular to the grain.

Comment: The factor 1.1 (=1.08) before $\sqrt{L/s}$ is ignored so that the equations also apply for $a = 0$.

The strong increase of the compression strength, up to at least a factor 5 as measured, or a factor 6 theoretically (by a local failure mechanism), is due to confined dilatation by hardening. Thus, the best experimental confirmation is obtained at a high inelastic strain when the empty spaces in wood are pressed away. It should not apply for plane stress at a stress-free boundary because there the uniaxial compression strength applies. However the factor c in:

$$\sigma_{c,90,u} = c \cdot f_{c,90} \sqrt{L/s}$$

is $c = 1.08$ for central loading and $c = 1$ for an end loaded block (when $a = 0$). and c can safely be taken to be $c = 1$ for all cases. The reason of this lack of difference in behaviour is the influence of the reinforcement, also perpendicular to the grain. The, by compression squeezed cell walls, act as additional reinforcement preventing the existence of continuous splitting planes in wood and providing a sufficiently strong reinforcement to build up confined dilatation quickly. This thus is an extension of the theory to stress-free boundaries, providing the simplification of the design rules with respect to the earlier CIB-W18 proposals.

Appendix B: Remarks regarding the availability of references

Each investigation is worth something and delivers something new but is incomplete when not explained by theory making it possible to connect all data of previous investigations and by that, to predict behaviour in all circumstances as necessary for design. Of importance is for example the approach of Bogensberger *et al.* (2011) providing the exact descriptive method of description of the loading curve by a flow rule with hardening properties. This opens future possibilities of theory development based on the real failure criterion as flow rule and may deliver by the hardening properties information on the real stress–strain rate behaviour according to molecular deformation kinetics at confined dilatation.

For the discussion here of the exact elastic-full-plastic solution according to limit analysis, very limited literature is available and only the oldest measurements, given for example by Figure 2, are sufficiently extended for theory verification. As mentioned, the theory, developed long ago is rigorous, a universal law of nature, and thus is able to explain and predict behaviour as necessary for a reliable design method and as shown here by the explanation of strength behaviour. The explanation and prediction of the strength of the North American ASTM-specimen database was repeated in 1991 at explaining the Korin (1990) data. In that respect, there is nothing new in later and recent publications of for example Blass and Gorlacher (2004) and Basta (2005) because the existence of the exact approach is not mentioned and ignored as guidance even though the power law approximation is much simpler to use than any empirical equation. Also the tests of Blass and Basta on the above mentioned ASTM-specimens were for example done 40 years ago and were repeated many times since then (see for example the relevant CIB-W18 publications) and

can be expected to still be repeated over 40 years because no progress is possible by the self-imposed omission of rigorous theory application. This is more the case because also the necessary elementary design of tests and test-specimens on the prediction of strength behaviour is lacking, Therefore, it is for example not noticed that the beams of Blass failed by shear and not by compression and his blocks, despite dimensions variation, all showed the same strength, by the same limited spreading possibility and thus no difference in spreading effect was tested. The tests of for example Basta on high longitudinal ends of beam-webs could have shown the full influence of the spreading effect in one direction when his longitudinal web length was enough extended according to the rolling shear strength pre-calculation. Due to the strict absence of theory and elementary calculation, mistakes and insufficiencies are not noticeable. Therefore, measurements without theoretical strength prediction in advance and theoretical explanation of the result afterwards, are meaningless for theory discussion. Based thereupon no reliable conclusion is possible.

In the article is shown again that application of the simple spreading equation as done in Section 3, to predict and explain all strength values of the different cases is sufficient.